



## Design and Testing of a Cabotegravir Implant for HIV Prevention

Dipu Karunakaran<sup>a</sup>, Solange M. Simpson<sup>a</sup>, Jonathan T. Su<sup>a,b</sup>, Ewa Bryndza-Tfaily<sup>c</sup>, Thomas J. Hope<sup>c</sup>, Ronald Veazey<sup>d</sup>, Georgina Dobek<sup>d,e</sup>, Jiang Qiu<sup>a</sup>, David Watrous<sup>a</sup>, Samuel Sung<sup>a</sup>, Jorge E. Chacon<sup>a</sup>, Patrick F. Kiser<sup>a,\*</sup>

<sup>a</sup> Department of Biomedical Engineering, Northwestern University, Evanston, IL, USA

<sup>b</sup> Department of Physics and Engineering, Elon University, Elon, NC, USA

<sup>c</sup> Department of Cell and Developmental Biology, Northwestern University, Chicago, IL, USA

<sup>d</sup> Division of Comparative Pathology, Tulane National Primate Research Center, Covington, LA, USA

<sup>e</sup> Tulane University School of Medicine, New Orleans, LA, USA

### ARTICLE INFO

#### Keywords:

Cabotegravir  
Subcutaneous implant  
Pre-exposure prophylaxis  
Hot-melt extrusion  
Hydrophilic poly(ether urethane)  
Reservoir device

### ABSTRACT

Long-acting antiretroviral implants could help protect high-risk individuals from HIV infection. We describe the design and testing of a long-acting reservoir subcutaneous implant capable of releasing cabotegravir for several months. We compressed cabotegravir and excipients into cylindrical pellets and heat-sealed them in tubing composed of hydrophilic poly(ether-urethane). The implants have a 47 mm lumen length, 3.6 mm outer diameter, and 200  $\mu\text{m}$  wall thickness. Four cabotegravir pellets were sealed in the membrane, with a total drug loading of  $274 \pm 3$  mg. *In vivo*, the implants released  $348 \pm 107$   $\mu\text{g}/\text{day}$  (median value per implant,  $N = 41$ ) of cabotegravir in rhesus macaques. Five implants generated an average cabotegravir plasma concentration of 373 ng/ml in rhesus macaques. The non-human primates tolerated the implant without gross pathology or microscopic signs of histopathology compared to placebo implants. Cabotegravir plasma levels in macaques dropped below detectable levels within two weeks after the removal of the implants.

### 1. Introduction

Implantable drug delivery systems provide durable drug levels to patients with suboptimal adherence to oral dosing regimens and demonstrably reduce pharmacological failure from missed doses [1,2]. All currently available small molecule antiretroviral (ARV) drugs for the prevention and treatment of HIV depend on a daily dosing schedule. Despite the user's desire to remain HIV negative, low adherence to daily ARV pre-exposure prophylaxis (PrEP) could be improved [3]. Furthermore, daily use ARV regimens can be particularly difficult for low-income individuals, those who do not have access to routine health care, and those who fear the stigma of being seen with anti-HIV medicines [4]. Improved adherence to HIV prevention dosage regimens and lasting protection from sexual transmission could have a significant impact on the global HIV pandemic [5].

Systemic long-acting ARVs to prevent and treat HIV infection has been extensively reviewed [6–9]. Several long-acting implants of tenofovir alafenamide fumarate [10–13] have been reported and an implant of Islatravir is advancing along the HIV prevention clinical-pipeline

[14,15]. Only a few ARVs are potent enough to fit a year's dose into a subcutaneous implant form factor and have slow enough elimination rates that a long duration implant can be achieved. Correspondingly, longer durations require high drug loading even with the most potent ARV, and, therefore, the implant design often requires a low mass fraction of polymeric component. Viable long-acting systems are achieved when the drug product combines potent and slowly eliminated pharmaceutical agents with biocompatible polymers that can control drug release [16,17]. Altogether, these design constraints demand as much from the formulation scientist, and the polymers used to make the implant as they do from the ARV.

The HIV integrase strand transfer inhibitor cabotegravir—(S/GSK1265744) [18–20] has been extensively studied as an injectable formulation of drug crystals. Cabotegravir is an insoluble molecule in water at pH 7.4 [21] and *in vivo* it is more than 99% plasma protein-bound. Studies of the cabotegravir suspension indicate an elimination half-life of 40 days in humans [21,22], and a single injection can have a duration of 1 to 2 months [23]. With oral cabotegravir, the drug has a metabolic elimination half-life of 40 h. Injectable cabotegravir was

\* Corresponding author.

E-mail address: [patrick.kiser@northwestern.edu](mailto:patrick.kiser@northwestern.edu) (P.F. Kiser).

<https://doi.org/10.1016/j.jconrel.2020.12.024>

Received 24 June 2020; Received in revised form 14 December 2020; Accepted 15 December 2020

Available online 19 December 2020

0168-3659/© 2020 Elsevier B.V. All rights reserved.

found to be more effective than oral tenofovir disoproxil fumarate-emtricitabine in preventing HIV infection [24]. The US Food and Drug Administration recently granted a Breakthrough Therapy designation to the cabotegravir injectable for HIV PrEP.

Recently, a refillable cabotegravir subcutaneous implant was reported by Pons-Faudoa and Grattoni [25]. The extensive knowledge gathered in the development of CAB oral and injectable formulations provides a rich set of inputs for the development of more advanced formulations. Notably, studies in non-human primates have reported the cabotegravir plasma level that correlates with complete protection from challenges with model immunodeficiency viruses [26]. Useful pharmacological characteristics of the drug are also available from human studies [21,26–29].

The injectable formulation of cabotegravir has a matrix-like pharmacokinetic (PK) profile with a broad peak followed by a long-tailed trough [26]. We hypothesized that a classical reservoir system might be able to diminish the burst phase, extend the duration of action at the same total dose of cabotegravir, and reduce the PK tail once removed. The pharmacokinetic tail is an essential parameter to consider since sub-therapeutic exposure in an infected unaware individual could potentially drive the development of resistant HIV strains. Upon implant removal, one can expect significantly lower terminal exposure to the ARV, and a shorter PK tail, as the source of the drug is removed.

Finally, the design of a practical subcutaneous implant must be driven by user needs while also keeping manufacturability in mind. Potential implant users order their device requirements around efficacy, convenience, duration, and privacy [30]. These different requirements impose design constraints on a practical subcutaneous implant. In an attempt to bridge these constraints, we investigated a modular capsule approach that would provide high drug loading and allow us multiple optimization cycles in the face of limited drug supply. The capsule was composed of a thin elastomeric-hydrogel membrane loaded with formulated pellets of drug substance that fit tightly in the extruded tubing. Herein, we describe the design, formulation development, and initial pharmacokinetic studies in non-human primates (NHP) of a cabotegravir reservoir implant.

## 2. Materials and methods

### 2.1. Materials

Cabotegravir, as the free acid (CAB H), CAS 1051375–10–0, and the sodium salt (CAB Na), CAS 1051375–13–3, in micronized and non-micronized forms, were provided by Viiv Healthcare Ltd. (Research Triangle Park, NC, USA). Medical grade hydrophilic poly(tetramethylene oxide) based poly(ether urethane) (HPEU) pellets, Tecophilic™ HP-60D-20 (Pathway™ PY-PT43DE20) and HP-60D-35 (Pathway™ PY-PT42DE35), were obtained from Lubrizol Advanced Materials (Wickliffe, OH, USA) and dried to less than 0.05% w/w of H<sub>2</sub>O before extrusion in house. The Pathway™ polyurethane polymers have extensive use in implantable medical devices and drug delivery systems. Master files for these polymers are available for reference through Lubrizol Corporation. Polyethylene Glycol 3350 USP NF was purchased from Fisher Scientific (Waltham, MA, USA) and dried to about 0.1% w/w of H<sub>2</sub>O before use. Kollidon™ 17 PF (Polyvinyl pyrrolidone, PVP K17 PF, weight average Mw 7000–11,000) was provided by BASF (Florham Park, NJ). Barium sulfate USP, magnesium stearate USP (Mg Stearate), and ethanol USP were obtained from Spectrum Chemicals (New Brunswick, NJ, USA). Rhodamine B isothiocyanate-Dextran 70 kDa (RITC-Dx) was obtained from Sigma-Aldrich (St. Louis, MO, USA). Acetonitrile (HPLC grade), sodium azide (ACS grade), methanol (HPLC grade), and Brij® 35 were obtained from Fisher Scientific (Fair Lawn, NJ, USA). 10× phosphate-buffered saline (PBS) and 10× TRIS buffered saline (TBS) from Fisher Scientific - were diluted to 1×, and the pH adjusted before use. Deionized (DI) water was obtained from a Thermo Scientific™ Barnstead™ E-Pure™ (Waltham, MA, USA) system. All

other chemicals and materials were purchased from Thermo Fisher Scientific (Waltham, MA, USA) and were HPLC or ACS grade when available.

### 2.2. Extrusion of the rate-controlling membrane

The manufacture of HPEU tubing was performed using methods similar to those described earlier [13,31]. In brief, tubing was manufactured from different HPEU for three different implant designs, referred to as A, B, and C. The rate-controlling membrane (RCM) tubing used for these were extruded with HP-60D-20, HP-60D-35, and a blend of 15% w/w PEG 3350 with 85% w/w HP-60D-35, respectively. The extrudate was air-cooled. The dimensions of the tubing extrudate were checked, and sections deviating greater than 10% from the target dimensions were rejected before use. The outer diameter of the tubing was measured with an ODAC 18 XY laser gauge (Zumbach Electronic, Orpund, Switzerland), and the wall thickness was measured with a spring-loaded digital caliper (Mitutoyo, Aurora, IL, USA).

HP-60D-20 tubing was extruded to an outer diameter of 2.2 mm and a wall thickness of 100 μm using a custom tubing crosshead (Guill Tool, West Warwick, RI, USA) attached to an ATR Plasti-Corder® single screw extruder (SSE) (C.W. Brabender, South Hackensack, NJ, USA). HP-60D-35 tubing was extruded on the SSE with an outer diameter of 3.6 mm and a wall thickness of 200 μm.

A polymer blend was used for the RCM in Implant C. PEG 3350 (15% w/w), and HP-60D-35 (85% w/w) were weighed out and blended. The blend was extruded to an approximately 2 mm diameter rod using a rod die on a C.W. Brabender KETSE 12/36 twin-screw extruder (South Hackensack, NJ, USA). The collected rod extrudate was pelletized with a micropelletizer (Randcastle Extrusion Systems Inc., Cedar Grove, NJ, USA). The resulting pellets were extruded into the tubing of outer diameter 3.6 mm and a wall thickness of 200 μm tubing with the SSE, which was fitted with a gear pump assembly (C.W. Brabender, South Hackensack, NJ, USA). A single channel lumen air system (Extrucore, Las Vegas, NV, USA) supplied air to prevent the hollow tube from collapsing as it exited the tubing die.

### 2.3. Manufacture of cabotegravir pellets

Drug containing pellets used in the-NHP studies were composed of CAB Na (~87%), PVP (~10%), and Mg stearate (~3%) made with the mill method described below. The drug substance was prepared by wet granulation, accomplished with a sieve or a mill. In the sieve method, CAB Na and PVP were weighed and mixed geometrically in a 90:10 weight ratio. The powder mixture was then wet granulated with ethanol, and the moist mass was forced through a No. 40 stainless steel mesh sieve to form granules. The moist granules were dried to constant mass using a ChemStar 1402 N vacuum pump (Welch Vacuum, Mt. Prospect, IL, USA). In the mill method, a cooled M 20 Universal mill (IKA, Wilmington, NC, USA) was used. Cabotegravir was massed and added to the precooled (14 °C) mill. A solution of the PVP in ethanol was added. The material was blended for two minutes, removed from the blender, and dried using the vacuum pump to constant mass. The dried material was processed in the precooled mill for a minute to break up aggregates.

The granules of CAB Na and PVP were lubricated by the addition of 3% w/w Mg stearate on a Labmill 8000 jar mill machine (Paul N. Gardner Company, Pompano Beach, FL, USA). The lubricated material was compressed into cylindrical pellets on an NP-RD10A semi-automatic tablet press (Natoli Engineering, St. Charles, MO, USA) at a force of 1000 lbs. with a multi-tip die punch set (Supplementary Fig. S1), forming four pellets every compression cycle.

Materials used in the formulation screening experiments were prepared by the wet granulation method described above or by geometrically dry mixing the components. Pellets of different diameters were obtained by changing the tablet punches and die. RITC-Dx pellets, used for the seal integrity testing, were manufactured by direct compression

of RITC-Dx using a 2 mm cylindrical multi punch/die set on the Natoli NP-RD10A semi-automatic tablet press. HP-60D-35 rods containing barium sulfate ( $\text{BaSO}_4$ , 40 wt%) were extruded as described previously [32] and cut to about 2 mm pellets for use as radiopaque pellets in the implants to facilitate imaging of implant location in rhesus macaques.

#### 2.4. Impulse sealing and implant assembly

The capsule ends were formed by thermal impulse sealing with a validatable computer-controlled sealer (PW2200, Packworld USA, Nazareth, PA, USA) shown in Supplementary Fig. S1. The tubing was first sealed at one end with the impulse sealer. Cylindrical CAB Na or CAB H pellets were then loaded into the tubing. A single HP-60D-35 pellet containing  $\text{BaSO}_4$ , approximately 2 mm long, was also loaded in devices manufactured for NHP studies. RITC-Dx pellets were added to some devices intended for leak testing. After loading the relevant pellet components in the core, the second end was sealed. The masses of hollow tubing, pellets, and the assembled implants were recorded in addition to the lumen length of the assembled implants. The implants were then annealed at 40 °C for 15–20 h to relieve any stress in the polymer generated during the impulse sealing operation.

The implant ends were sealed using controlled sealing temperature ( $T_s$ , °C), sealing time ( $t$ , s), jaw pressure ( $P$ , psi), and cooling temperature ( $T_c$ , °C). The sealing conditions used for Implant A, manufactured with HP-60D-20 tubing, was  $T_s = 180$  °C,  $t = 6$  s, cooled to  $T_s = 50\%$ ,  $P = 60$  psi. The sealing conditions used for Implants B and C, manufactured with HP-60D-35 tubing, was  $T_s = 185$  °C,  $t = 98.9$  s,  $T_c = 37$  °C,  $P = 10$  psi. Before sealing either end, the ends were thoroughly cleaned with swabs and the use of pressurized air from a compressed air can. The conditions used to form the seal and determine sealing conditions that generate robust seals were performed as described earlier [13] or by following the mass of the implants. A failure of the seals was noticed when there was a drop in the mass of the hydrated implant.

Implants manufactured for the NHP studies were placed in metalized pouches (U-line, Pleasant Prairie, WI, USA) after assembly and sealed with a heat sealer (AIE-300CA, American International Electric, City of Industry, CA, USA) in ambient air. The sealed pouches were placed at 40 °C for 15–20 h before being shipped for electron beam (e-beam) sterilization with 25 kGy of irradiation at Steri-Tek (Fremont, CA, USA).

While the implants destined for NHP studies were manufactured in a non-sterile environment, utmost care was taken to depyrogenate contact surfaces and minimize contamination during manufacturing, as described previously [33]. Endotoxin testing, using reported methods [32], was performed on raw materials and the e-beam sterilized implants.

#### 2.5. Cabotegravir LC method

Cabotegravir levels were measured using an Agilent 1200 series high-performance liquid chromatography (HPLC) system equipped with a diode array detector. Cabotegravir was monitored at a wavelength of 260 nm. A Zorbax Eclipse XDB C18 column ( $4.6 \times 150$  mm, 5  $\mu\text{m}$ , Agilent) with a Zorbax Eclipse XDB-C18 guard column ( $4.6 \times 12.5$  mm, 5  $\mu\text{m}$ , Agilent) was used for separation. The column thermostat was set to 25 °C. Mobile phases used were A: 0.1% trifluoroacetic acid (TFA) ( $v/v$ ) in water and B: 0.1% TFA in acetonitrile (ACN). Cabotegravir content in release media was assayed using an isocratic method of 60% A and 40% B over 10 min. In stability studies, Cabotegravir was quantified using a gradient method (0 min - 85% A, 2 min - 85% A, 12 min - 5% A, 15 min - 5% A, 15.1 min - 85% A, 20 min - 85% A, total run time was 20 min). The flow rate of the mobile phase was 0.8 ml/min. CAB Na standards were prepared in methanol at 5  $\mu\text{g/ml}$ , 50  $\mu\text{g/ml}$ , and 200  $\mu\text{g/ml}$  and injected at 1  $\mu\text{l}$ , 2  $\mu\text{l}$ , 5  $\mu\text{l}$ , and 10  $\mu\text{l}$  volumes to generate the twelve point calibration curve.

#### 2.6. In vitro release testing

*In vitro* release tests (IVRT) were performed in 40 mL glass vials, with the release media changed daily. The vials were placed in a New Brunswick model I26 stackable incubator shaker (Eppendorf Bio Tools, Hauppauge, NY, USA) maintained at 37 °C and shaken at 80 RPM. Sink conditions were maintained (CAB Na released concentration < 20% of the maximum solubility in release media) over the course of all studies. At the sampling points, a portion of the release media was collected and analyzed by the HPLC method described above to determine the daily release rate. Long term release studies were performed in TBS buffer (25 mM Tris, 2.7 mM KCl, 137 mM NaCl) with 2%  $w/v$  Brij 35, buffered to pH 8.0 and containing 0.02%  $w/v$  sodium azide. The collected release samples were diluted with ACN, three parts sample and two parts ACN, immediately after collection and promptly analyzed. Some screening studies utilized a release media consisting of PBS buffer (0.137 M NaCl, 0.0027 M KCl, and 0.0119 M phosphates, pH 7.4) with 2%  $w/v$  sodium dodecyl sulfate (SDS) and 0.02%  $w/v$  sodium azide and are noted in figure legends.

The pH, osmotic pressure, and Cabotegravir concentration of the liquid inside fully hydrated implants ( $n = 5$ ) placed in PBS were determined. The internal contents recovered from the hydrated implant were centrifuged and passed through a 0.2  $\mu\text{m}$  syringe filter. A pH micro-electrode (Mettler-Toledo, Columbus, OH) was used to measure the pH on low volume samples. The osmotic pressure was determined with a vapor pressure osmometer (Vapro model 5520, Wescor, Logan, UT, USA). Cabotegravir concentration was measured with the HPLC method described earlier.

#### 2.7. Preliminary formulation experiments

Test devices were manufactured with non-micronized forms of CAB H or CAB Na to determine the best salt form to be used in the core of the implant. Solubilizing agents commonly used in parenteral formulations were screened for their effect on cabotegravir release rate and swelling effects on the device. Non-micronized cabotegravir in HP-60D-20 tubing was used with the concentration of solubilizing agent set at 7.5%  $w/w$ . The average drug release and swelling values were collected and compared once the implants were fully hydrated (between days 10–15). Devices were also manufactured with micronized cabotegravir. Devices were made with increasing PVP K17 PF concentration using micronized cabotegravir. HP-60D-35 tubing was used for these later studies. Finally, three prototypes of the devices were manufactured, for further study. Five devices were tested during each *in vitro* release study, and the values are reported as mean  $\pm$  SD.

The compositions of key formulations are provided below. Implant A, HP-60D-20 tubing, outer diameter (OD) 2.2 mm, wall thickness (WT) 100  $\mu\text{m}$ , lumen length (LL) 21 mm, core formulation pellet composed of CAB Na (non-micronized):PVP K30:Mg Stearate weight ratio 87:10:3, CAB Na strength 52 mg; Implant B, HP-60D-35 tubing, 3.6 mm OD, 200  $\mu\text{m}$  WT, 47 mm lumen length, core formulation pellet manufactured with CAB Na (micronized):PVP K17 PF:Mg Stearate weight ratio 87:10:3, Cabotegravir strength 275 mg; Implant C, HP-60D-35/PEG 3350 (85/15 weight ratio), 3.6 mm OD, 200  $\mu\text{m}$  WT, 47 mm lumen length, core formulation pellet was CAB Na (micronized): PVP K17 PF: Mg Stearate weight ratio 87:10:3, Cabotegravir strength 275 mg. A complete table of all formulation used in the manuscript is given in the Supplemental Table S4.

#### 2.8. X-ray diffraction studies

XRD data were collected at room temperature on an STOE-STADI-P powder diffractometer (Darmstadt, Germany) equipped with an asymmetrically curved germanium monochromator ( $\text{CuK}\alpha_1$  radiation,  $\lambda = 1.54056$  Å) and MYTHEN2 1 K one-dimensional silicon strip detector (DECTRIS, Dättwil, Switzerland). The line focused Cu X-ray tube was

operated at 40 kV and 40 mA. CAB Na powder or pellets were packed in an 8 mm metallic mask and sandwiched between two polyimide layers of tape and measured while rotating in transmission scan mode. For analyzing the implant which had been used for *in vitro* release studies, the implant was first patted dry, placed between the sample holder and an 8 mm metallic mask, and measured parallel to the detector without rotation in transmission scan mode. The material within the explanted implant after a 12-week PK study was also analyzed. The core material from this implant was loaded into a boron rich glass capillary tube (Charles Supper, Natick, MA, USA), placed in a capillary holder and the measurement obtained in Debye-Scherrer scan mode. The instrument was calibrated against a NIST Silicon standard (640d) prior to measurements.

## 2.9. Effect of changing implant length

HP-60D-20 tubing with a wall thickness of 100  $\mu\text{m}$  was used in studies to determine the influence of geometrical factors on the release rate. The manufactured implants ranged in lumen length from about 11 mm to 37 mm ( $n = 10$ , 11.4 mm;  $n = 5$ , 16.2 mm;  $n = 9$ , 21.3 mm,  $n = 10$ , 37.0 mm). Release rates were averaged between days 10–50.

## 2.10. CPartition measurements

Films of HP-60D-20 and HP-60D-35 were placed in CAB Na saturated solution of PBS containing PVP K17 and incubated at 37 °C for two weeks. After removal, the films were rinsed in DI water and wiped dry with lint-free paper. The films were then dissolved with dimethylacetamide in a volumetric flask. Methanol was added to precipitate the polymer, and the filtered supernatant was analyzed by HPLC. The concentration of CAB Na in the incubating solution was also determined. Control samples of the polymers were processed similarly to test samples, but with the addition of a known amount of CAB Na spiked in the samples. Partition coefficients were expressed with the following equation.

$$K = \frac{c_p}{c_c} \quad (1)$$

where  $c_p$  is the saturated concentration of cabotegravir in the polymer membrane phase and  $c_c$  is the concentration of drug in the solution phase.

## 2.11. Release from cabotegravir implants after e-beam sterilization

CAB Na implant A was subjected to e-beam sterilization at 25 kGy (Steri-Tek, Fremont, CA, USA). The sterilized implants were placed on IVRT. The release of cabotegravir from the sterilized implants was compared with that from non-sterilized implants to study if the sterilization procedure affected the release profile.

## 2.12. Preclinical pharmacokinetic and safety studies

The studies in rhesus macaques were performed adhering to protocols approved by Tulane National Primate Research Center local institutional animal care and use committees (Tulane protocol P0307R). The study was carried out under the Guide for the Care and Use of Laboratory Animals of The Institute of Laboratory Resources, National Resource Council. All procedures were performed under anesthesia using ketamine/xylazine, and every effort was made to minimize stress, improve housing conditions, and provide enrichment opportunities. When necessary, macaques were euthanized by sedation with ketamine/xylazine injection followed by intravenous barbiturate overdose in accordance with the recommendations of the panel on euthanasia of the American Veterinary Medical Association.

## 2.13. The surgical subcutaneous implantation procedure

The macaques were anesthetized before surgery. Baseline blood samples, along with vaginal and rectal swabs, were collected. The implants were inserted between the shoulder blades. A small incision was made in the skin, and a trocar (Elemis Corp., Carson City, NV) was gently inserted under the skin to create a site for the implant. The number of incisions made depended on the number of implants being tested. A monthly schedule for sampling is provided in Table 1. Macaque implant details are shown in Supplementary Table 1.

## 2.14. Blood collection and bioanalytical procedure

Blood samples were collected before the devices were implanted, and after that at specified time intervals for at least 12 weeks. Approximately 8 ml of blood was taken from the femoral vein, transferred into EDTA-coated tubes, and immediately placed on ice. The tubes were centrifuged (2100 rpm, 20 min, 4 °C) to separate plasma from cells. The isolated plasma was transferred to new tubes and stored at –80 °C. Cabotegravir was quantified using a validated LC-MS method [25] at the Clinical Pharmacology Analytical Laboratory of Johns Hopkins University School of Medicine. The lower limit of quantification was 25 ng/ml for plasma samples. Additionally, 1 ml of blood was collected before the surgeries and every four weeks for blood chemistry studies.

## 2.15. Vaginal and rectal biopsy collection

Tissue samples of vagina and rectum were collected in 15 or 50 ml vials. The samples were trimmed into 50–250 mg tissue pieces, weighed, transferred into 1 ml cryovials, immediately frozen and stored at –80 °C for analysis later with a validated LC-MS method [25] at the Clinical Pharmacology Analytical Laboratory of Johns Hopkins University School of Medicine. The lower limit of quantification was 0.05 ng/sample for tissue samples [25].

## 2.16. Extraction of residual drug from explanted implants

**Section 2.16-**During manufacturing the initial mass of drug in each implant was recorded. In total, 41 implants (4.7 cm, implant B) were recovered from NHP, extracted and analyzed for residual cabotegravir. The results of the extractions appear in Table S3. Each explanted implant was trpsinized for two minutes, -and the fibrous capsule removed with a pair of tweezers. Images of the implants, before and after tissue removal, were collected. The seal integrity was checked visually, followed by compressing the implant and observing for compression-induced fluid expulsion. The implant was frozen, sliced open, the residual drug extracted with methanol, and analyzed using the HPLC method described above. Control implants with known loadings were also extracted, with recovery of  $99 \pm 1.2\%$  of the loaded drug ( $N = 5$ ).

## 2.17. Implant site histology

At 4 and 12 weeks post-implantation, two macaques were euthanized after collecting blood samples, vaginal and rectal fluids. Samples of vagina, rectum, and tissue around the implant site were collected fresh, aliquoted, weighed, and frozen at –80 °C for later HPLC analysis of cabotegravir levels. As described earlier [32], the entire implant site was carefully dissected intact, pinned onto paraffin blocks, and fixed in place with z-fix. Multiple paraffin-embedded sections of collected tissues were examined histologically for signs of the presence and severity of inflammation by staining with hematoxylin and eosin (H&E). Samples were blinded and examined by a trained pathologist. The thickness of the fibrous capsule surrounding the implant was measured using -ImageJ [34].

**Table 1**  
NHP study schedule.

Procedure	Time (weeks)												
	0	1	2	3	4	5	6	7	8	9	10	11	12
Implantation	x												
Blood sample	x	x	x	x	x	x	x	x	x	x	x	x	x
Vaginal swabs	x		x		x				x		x		x
Rectal swabs	x		x		x				x		x		x
Vaginal biopsy					x				x				
Rectal biopsy					x				x				
Necropsy					2 NHP								2 NHP

### 3. Results and discussion

#### 3.1. Implant manufacturing

This implant design was chosen because it is a modular approach that would allow the implant features to be individually modified and tested without using excessive quantities of the drug substance. Many factors influenced the feasibility of early prototypes, including sealing methods for HPEU membrane capsules. It was observed that impulse sealing of water-swellaible HPEU required care since the material interface was stressed by the initial transient shear stresses when swelling occurs and then by osmotic forces that pressurized the implant. Delamination of the seal was observed when implants were placed in an aqueous solution if the bond between the two seal surfaces was weak. Therefore, extensive experiments were conducted to define a suitable temperature and sealing time design space where robust seals can be produced. Maximum temperatures were selected for these experiments by identifying the temperature at which bubbling or discoloration of the polymer interface occurred. The minimum temperature was the temperature where the seal could not be delaminated by hand. For HP-60D-35, these temperature limits were 185 °C and 80 °C (Fig. S2). A wide range of temperature/time combinations was scanned (see Supplementary material), and it was found that implant B sealed at  $T_s = 185$  °C,  $t = 98.9$  s,  $T_c = 37$  °C,  $P = 10$  psi resulted in implants that retained seal integrity *in vitro* (Fig. S2). These implants survived repeated compressive stress tests (Fig. S3). Other sealing methods were explored in preliminary studies (Fig. S4).

#### 3.2. Implant design constraints

This project started with a set of user-driven and practical design constraints that aimed to minimize the number of implants and their size. Exploratory studies - on cabotegravir diffusion through polymer membranes used various elastomeric polymers (poly(dimethylsiloxane), poly(ethylene-co-vinyl acetate), and segmented -HPEU. We were only able to achieve pharmacologically useful fluxes of cabotegravir from -HPEU hydrogels (Supplementary Table S2). We selected the -HPEU HP-60D-35 - that swells in water approximately 40% by weight as an acceptable tradeoff between dimensional change after swelling and drug permeability. The thinnest consistent wall thickness of HP-60D-35 we could repeatedly manufacture with our extrusion equipment was between 150 and 200  $\mu$ m. We selected the outer diameter of the implant as 3.6 mm because it could easily be inserted through a commercially available trocar. A 200  $\mu$ m thick RCM and a 100  $\mu$ m gap to allow core pellet insertion into the tubing, therefore, set the core pellet diameter for further studies at 3.0 mm.

We found empirically we could readily place four 1 cm long cylindrical pellets within a 4.7 cm lumen length tube (total tube length  $\sim$  6.1 cm) and seal these with our impulse sealing instrument. This implant can be delivered to the subcutaneous site with the commercially available trocar we selected for NHP studies. The CAB Na pellets had a density of 1.24 g/ml. With an implant lumen length of 4.7 cm, this implant would have an internal volume of approximately 0.3 ml and

allow loading on the order of  $\sim$ 300 mg of CAB Na.

#### 3.3. Effect of pellet composition on drug release

The solubility of CAB H in water and PBS (pH 7.4) is 6.2  $\mu$ g/ml and 9.5  $\mu$ g/ml, respectively. The corresponding values for CAB Na are 231.6  $\mu$ g/ml and 312.0  $\mu$ g/ml in water and PBS (pH 7.4), respectively. Prototype implants made with CAB Na showed a significant increase in drug flux over those made with CAB H ( $p < 0.0001$ , Fig. 1b). Since cabotegravir is slightly soluble in water, a water-soluble excipient was added to - osmotically drive fluid into the core of the implant and subsequently cause disintegration of the pellet and solubilization of cabotegravir in the core of the implant. We screened a series of formulations with different excipients in the core (Fig. 1c). Although implants with PEG 3350 had the highest average release rate at 0.21 mg/cm/day, these implants had a higher swelling ratio ( $m_w/m_d$ ) of 3.2 compared to the others. The PEG 3350 has a lower molecular weight than PVP K30 and therefore has the potential to provide a higher osmotic pressure gradient in the core of the implant than PVP K30 when solubilized. We aimed to achieve a high release rate while attempting to keep the implant swelling low. PVP was selected as an excipient for further study because PVP containing implants had a lower mass swelling, a high release rate, and PVP has a history of human parenteral exposure in multiple products.

PVP is available in a parenteral grade that is free of pyrogens. In follow-on studies, we found PVP K30 (MW  $\sim$  40,000) and PVP K17 PF (MW  $\sim$  9000 g/mol) produced similar release curves over a month of IVRT ( $f_2 = 90$ ) - [35,36] - (Fig. S7). Furthermore, PVP K17 has a lower molecular weight than PVP K30 and could be eliminated if an implant leaked its contents [37]. A series of formulations were made with increasing fractional PVP K17 PF content. The 10 wt% provided the maximum release rate (Fig. 1d), with no observed advantages above this concentration. Hence, 10% (wt) was chosen as the formulation composition with 3% magnesium stearate (as a lubricant during pellet compression) to maximize drug loading and release. We also confirmed that micronized CAB Na increases the release rate in HP-60D-35 tubing ( $p = 0.027$ , Fig. 1e), compared to the non-micronized form.

We attempted to increase the release rate further by adding a water soluble porogen PEG 3350 [38] to the HP-60D-35 membrane material. We found that blend compositions above 15 wt% PEG 3350 were challenging to extrude, with the extrudate tending to promptly collapse upon exiting the die, even with attempts to improve cooling or support the lumen with air pressure. We did observe a modest increase in the cabotegravir release rate in the presence of the PEG porogen (Figs. 1f, 2a). However, to reduce complexity and ease of manufacturing, we proceeded with further characterization of the implant composed solely of the HP-60D-35 HPEU.

#### 3.4. Implant characterization

With an optimized formulation composition in hand (Table 2), we conducted several studies to characterize the prototype implant. Release rates for three different implants were determined (Fig. 2a) in TBS, pH

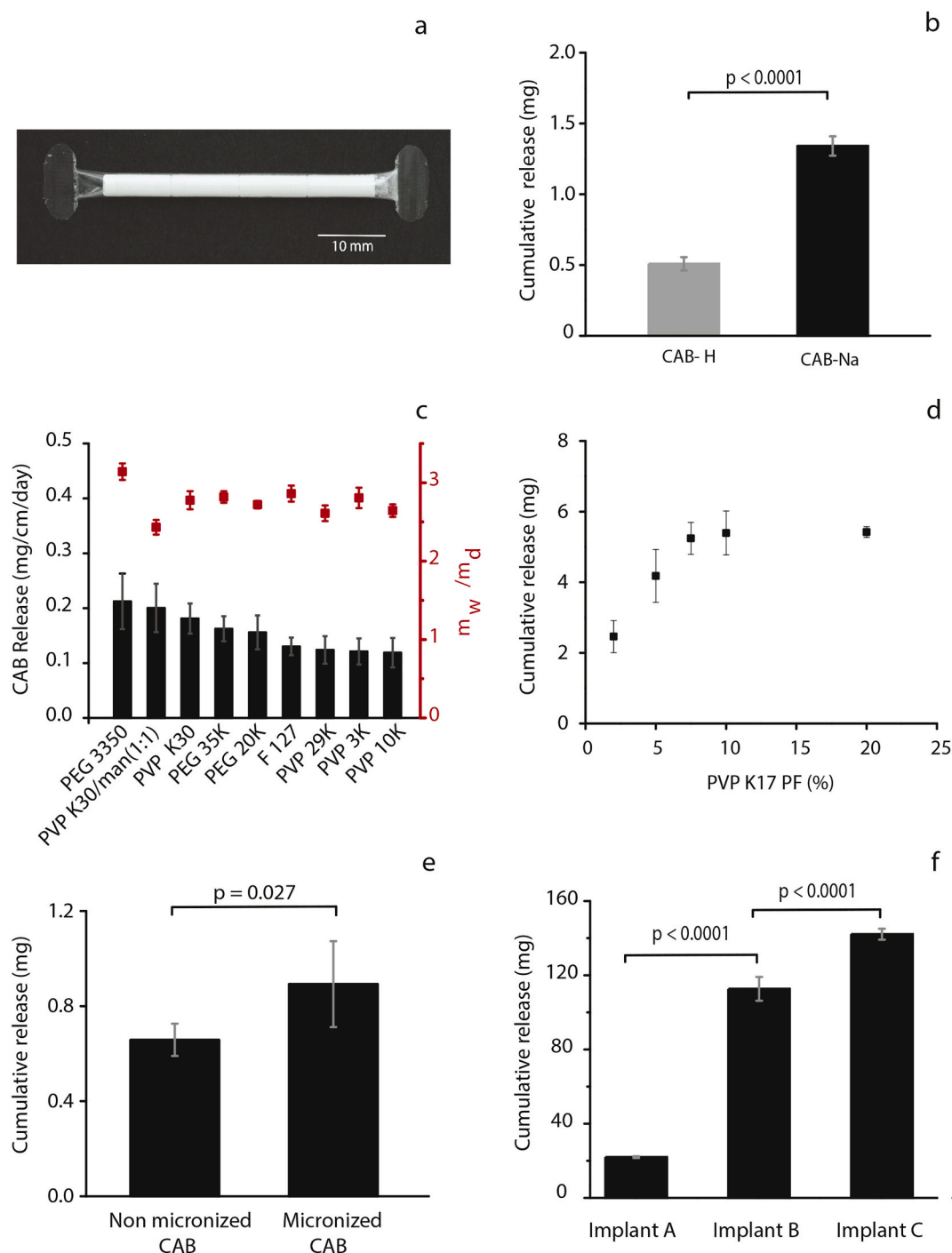


**Fig. 1.** Formulation development studies. (a) CAB Na implant B (b) Difference in cumulative release of CAB Na and CAB H implants (c) Effect of solubilizers in the implant core on release rate (average between days 10–15) (d) Effect of PVP K17 concentration (20-day data) (e) Micronized CAB Na increased release rate (16-day data) (f) Comparison of cumulative release rate of three CAB Na implants (232 days).  $N = 5$ , error bars are standard deviations, details in Section 2.7.

8.0. In this release media, the release curve appears to be biphasic that asymptotes to a plateau value over 80 days. Once hydrated by the release media, the solid core, which is ~87% drug by mass, provides a source of the undissolved drug to maintain saturated conditions within the reservoir, driving drug release through a concentration gradient across the RCM. The implant's release rate can be adjusted through the modulation of the geometry of the HPEU RCM. The linear data, when a plot of the release rate against the geometric factor  $2\pi l / \ln(r_o/r_i)$  [13] is constructed (Fig. 2b), suggests that the daily dose can be tuned based on the overall length of the implant and, radius and thickness of the RCM.

At pH 8.0, in the IVRT media, XRD data indicates that there is acid-base disproportionation of the Na<sup>+</sup> salt to the free acid slowly over time in the aqueous media inside the implant. The spectra for CAB H, CAB Na, material recovered from the core of the implant after 3 weeks in release media, and cabotegravir pellet formulation (pre hydration) are shown in Fig. 2c. CAB H and CAB Na have characteristic peaks at 5.3° and 6.7°, respectively. When CAB Na was wet granulated with ethanol, some of the higher spectra were absent. After three weeks of exposure to release media, the pellets in the implant core were observed to be completely hydrated. Scattering at 5.3°, which was absent in the dry CAB Na pellet

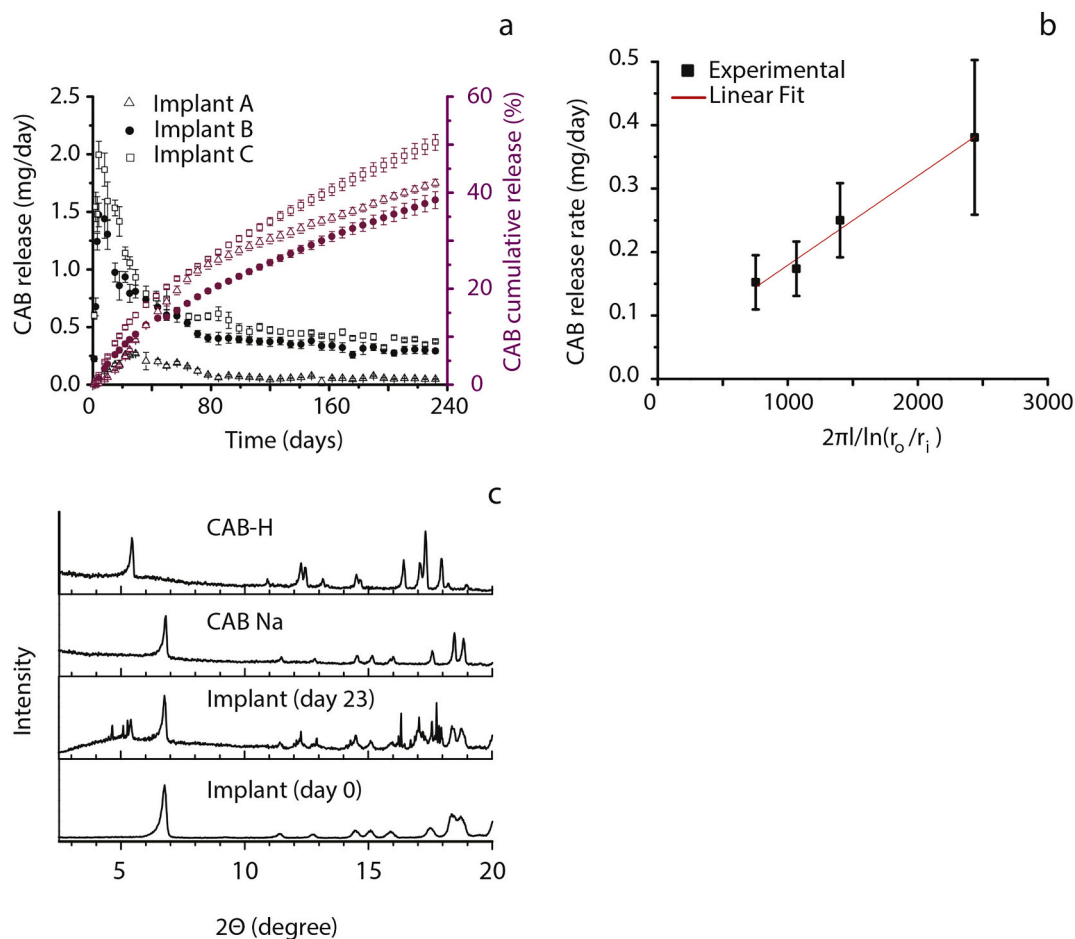


**Fig. 2.** *In vitro* release studies. (a) Daily and cumulative *in vitro* release of three different CAB Na implant formulations,  $n = 5$ , details in Section 2.7. (b) Release rate of with change in implant dimension,  $R^2 = 0.927$ , error bars are  $\pm$  standard deviation, Implant B core and HP-60D-35 wall, details in Section 2.9 and Table S4. (c) XRD spectra of a hydrated implant.

**Table 2**  
Implant B description.

	Total mass of implant	$\sim 440$ mg
	Strength of implant	274 mg of CAB Na
Tubing	Wall material	HP-60D-35
	Wall thickness	200 $\mu$ m
	Outer diameter	3.6 mm
	Lumen length	47 mm
	Tubing mass	145 mg
	Pellet	Pellet composition
	Pellet diameter	3 mm
	Pellet length	10 mm
	Pellet mass	80 mg
	Number of pellets	4

formulation, was present in the dried post hydration sample. These data suggest that within the core of the implant, the sodium salt of cabotegravir converts to the free acid during *in vitro* release testing. Disproportionation of cabotegravir is one factor that could account for the changing release rate of the drug.

We characterized the pH, osmotic pressure, concentration of cabotegravir in the core of the implant, and the swelling of the implant when placed in PBS. After 30 days, the concentration of cabotegravir within the implant core fluid was  $277 \pm 12$   $\mu$ g/ml, and the internal pH was 8. The corresponding concentration and pH for the PBS media in which the implant was placed was  $148 \pm 7$   $\mu$ g/ml (cabotegravir concentration) and

7.7 (pH). The osmotic pressure in the core was  $281 \pm 12$  mOsm/kg, and in the external media, it was  $259 \pm 7$  mOsm/kg (all values mean  $\pm$  SD,  $n = 5$  implants). The implant core creates a 22 mOsm/Kg osmotic pressure gradient and a pH gradient of 0.3 pH units between the core and the external environment ( $p < 0.002$  for osmotic pressure measurements and  $p < 0.0001$  for pH measurements).

We were also interested in the presence of cabotegravir concentration gradients in the core of the device and the membrane. The concentration of cabotegravir in HP-60D-35 and HP-60D-20 films after incubating them in a saturated cabotegravir solution of pH 7.4 PBS containing the implant core excipient PVP K 17 PF, was determined to be  $1.7 \pm 0.1$  mg/ml and  $1.3 \pm 0.1$  mg/ml ( $n = 5$ ), respectively. The concentration of cabotegravir in the incubating solution was  $396 \pm 15$   $\mu$ g/ml ( $n = 10$ ). Cabotegravir partitions and concentrates to a level as much as  $K = 4.3$  times the concentration in the core simulant media in HP-60D-35. The partitioning coefficient was lower for HP-60D-20—a lower swelling copolymer variant of HP-60D-35—with a value of  $K = 3.4$ .

When placed in PBS medium, or the subcutaneous space in macaques, PVP K17 PF containing implants fill with liquid. The implants also change dimensions -in water because they are composed of elastomeric hydrogels that isotropically swell and -conduct water through the membrane. Additionally the implants are loaded with a modest weight fraction of water soluble polymer-(PVP) that creates a chemical potential gradient of water across the membrane. Additionally the implant also expands during hydration from the corresponding osmotic pressure gradient that places the membrane under tension. In PBS, pH 7.4, we observed that the implant B swelled over ten days to approximately two

times its initial mass (Fig. S3) and maintained that degree of swelling. Implant B started with a dry mass of  $540 \pm 18$  mg (SD,  $N = 5$ ) to  $1118 \pm 70$  mg (SD,  $N = 5$ ) when hydrated. Implant B began at 3.6 mm in diameter and 4.7 cm long when dry and swelled to a diameter of 4.9 mm and a length of 6.0 cm when hydrated.

Inside the implant, we observe that the pellet disintegrates in approximately two weeks into a cabotegravir solid suspension. We subjected implants to a cyclical mechanical stress test (see Supplemental material) and saw no evidence by HPLC of leaking of the core material when placed under compression. Furthermore, we found the HPEU implants are mechanically robust and could withstand repeated deformation without failure.

Together these data suggest a series of events drive the release of cabotegravir from the implant. When placed in aqueous media, the water-swellaible RCM mixes with water and swells like other hydrogel network polymers [31]. An osmotic gradient from wetted and solubilized PVP and cabotegravir in the core drives more external aqueous liquid into the implant, and the implant fills with this ultrafiltered solution and places the elastic membrane under tension. Hydration of the internal contents begins the process of disintegration of the core pellet, increasing the wetted surface area of cabotegravir. The drug is soluble in the implant fluid to some degree, but it also partitions into the membrane at  $\sim 4\times$  higher concentration. The difference between the membrane concentration and the concentration in the external media creates the concentration gradient that drives drug release. The implant remains swollen with the membrane under tension for at least 250 days, suggesting that PVP maintains an osmotic gradient in the core for the life of the implant. Over time because the pKa of cabotegravir (pKa = 7.71) [39] is near the media pH, cabotegravir disproportionates to a mixture of the free acid CAB H and the ionized form of the drug.

### 3.5. Pharmacokinetics in rhesus macaques

We designed an exploratory macaque PK and safety study where both active and placebo implants were contralaterally implanted on the dorsal back in three pockets as described elsewhere [32]. Since we wanted to track the location of the implants during *in vivo* PK studies, HPEU pellets containing 40 wt% BaSO<sub>4</sub> were included in the implant core, and these could be easily imaged through radiography of the macaques (Fig. 3a, arrows). Utilizing cabotegravir implant B, we conducted a PK study in rhesus macaques with an increasing dose of cabotegravir by increasing the number and length of implanted devices. We investigated five groups of macaques: G1, four macaques with two 3.1 cm active implants and a matched placebo, G2 had four macaques with two 4.7 cm active implants and one placebo; and G3 had four 4.7 cm active implants, G4 had five 4.7 cm active implants, and G5 had six 4.7 cm active implants with three rhesus macaques within each group G4-G5. In G1 and G2, one macaque from each group was necropsied at one month and another at three months for tissue samples and local histopathology of the active and placebo implantation site. All other macaques were explanted and placed back in the colony after a drug washout period.

The pharmacokinetic profiles in all five groups displayed median C<sub>max</sub> in the first two weeks (first quartile (Q1) - two weeks, third quartile (Q3) - four weeks) of exposure with reducing levels that appear to plateau at longer times (Fig. 3b). Total cabotegravir exposure generally followed an increasing linear trend with total implant lumen length (Fig. 3c, G1-G5, Pearson's  $r = 0.885$ ) but appeared to saturate at a total lumen length of 18 cm. The cabotegravir plasma levels from the five implant study group were close to those reported by Ho et al. [40] as providing complete protection from repeated low dose rectal immunodeficiency virus challenge. Other data in rhesus macaques [41] suggest that a plasma cabotegravir level of approx. 150 ng/ml could protect greater than 90% of intravaginally challenged macaques with a high dose of simian-human immunodeficiency virus.

Interestingly, we observed that the 6-implant group had lower means

and median cabotegravir exposure (Fig. 3e). Although the study has low power, we speculate that this may indicate two implants next to each other could interfere with mass transport of drug from the implant and into the bloodstream by saturating the tissue around the implant with cabotegravir. By extracting 41 implants (Implant B), we found the average release rate over the 12 week period to be  $348 \pm 107$   $\mu\text{g/day}$  (median value per implant,  $N = 41$ ) of cabotegravir (Table S3). This represents 11% of the total initial loading in 90 days. Post implant removal, the plasma cabotegravir levels fell below the limit of detection (25 ng/ml) for almost all the tracked macaques by week two (Fig. 3h). The average plasma half-life for the devices is approximately nine days. Rectal biopsies had median levels of 61 ng/g (Q1–36 ng/g, Q3–105 ng/g) at week 12 (Fig. 3g), a value lower than seen in the injectable formulation [41] where macaques were injected with 10 mg/kg or 30 mg/kg.

We encountered implant loss in two macaques in different groups. One macaque in G5 lost an implant, and another in G6 lost three. Loss of implants appeared to be macaque-specific, and the macaques may have explanted the implants through grooming. The intact explanted devices from the PK study were coated in a transparent and mechanically robust fibrous capsule (Supplementary Fig. S5). Mechanical testing of explanted devices indicated that all explanted HPEU membranes were intact. Furthermore, the *in vitro* release rate was similar before and after explantation. Our *in vitro* release method with the TBS media and the release rate of the drug *in vivo* could be used to develop an *in vitro-in vivo* correlation to aid further implant research (Fig. 3d).

Since we observed evidence of the disproportionation of CAB Na during *in vitro* studies, we investigated if explanted devices had X-ray spectra that indicate the presence of the free acid form of cabotegravir. The XRD spectra of the internal contents of a recovered implant (Fig. 3f) suggest that the CAB Na formulation undergoes disproportion *in vivo*. Given the much lower release rate of CAB H formulations (Fig. 1b), this finding would suggest that increasing the internal pH of the cabotegravir implant could increase overall drug release by increasing drug solubility.

### 3.6. Local histopathology

Fibrous tissue encapsulation is the end-stage response to a foreign body [16,32]. We found a fibrous capsule surrounding the retrieved implants in all explanted devices. The capsule could be removed by proteolysis with trypsin and pulling away the membrane with forceps. Overall, the response to the placebo and active implants appears similar at the gross level and microscopic length scales. The macaques generally appeared healthy with stable blood chemistry, weight, and behavior. Histology of the active and placebo implantation sites was normal (Fig. 4a-d). The difference of fibrous capsule thickness around the active and placebo macaques was insignificant (Fig. 4e,  $p = 0.38$  at four weeks,  $p = 0.67$  at 12 weeks). Some have expressed concerns about the crimped edges causing increased fibrosis at the ends of the device. We saw no evidence in tissue sections taken along the length of the cabotegravir implant. Similar placebo implants matched to an implant system for a different drug [32] also showed no evidence of increased fibrosis or scarring at the ends of this implant design. As described in our recent publication [32] and the guidance for local inflammation studies in the implanted device described in ISO 10993-6 [42], it is essential to retrieve the implant with intact surrounding tissue to assess local histopathology of implanted devices accurately. A careless recovery of the implanted device before fixing the tissue disturbs the surrounding cellular structures induced by inflammation, making it impossible to interpret signs of local histopathology.

## 4. Conclusion

We describe a subcutaneous reservoir implant capable of delivering approximately 350  $\mu\text{g/day}$  of cabotegravir over three months in rhesus

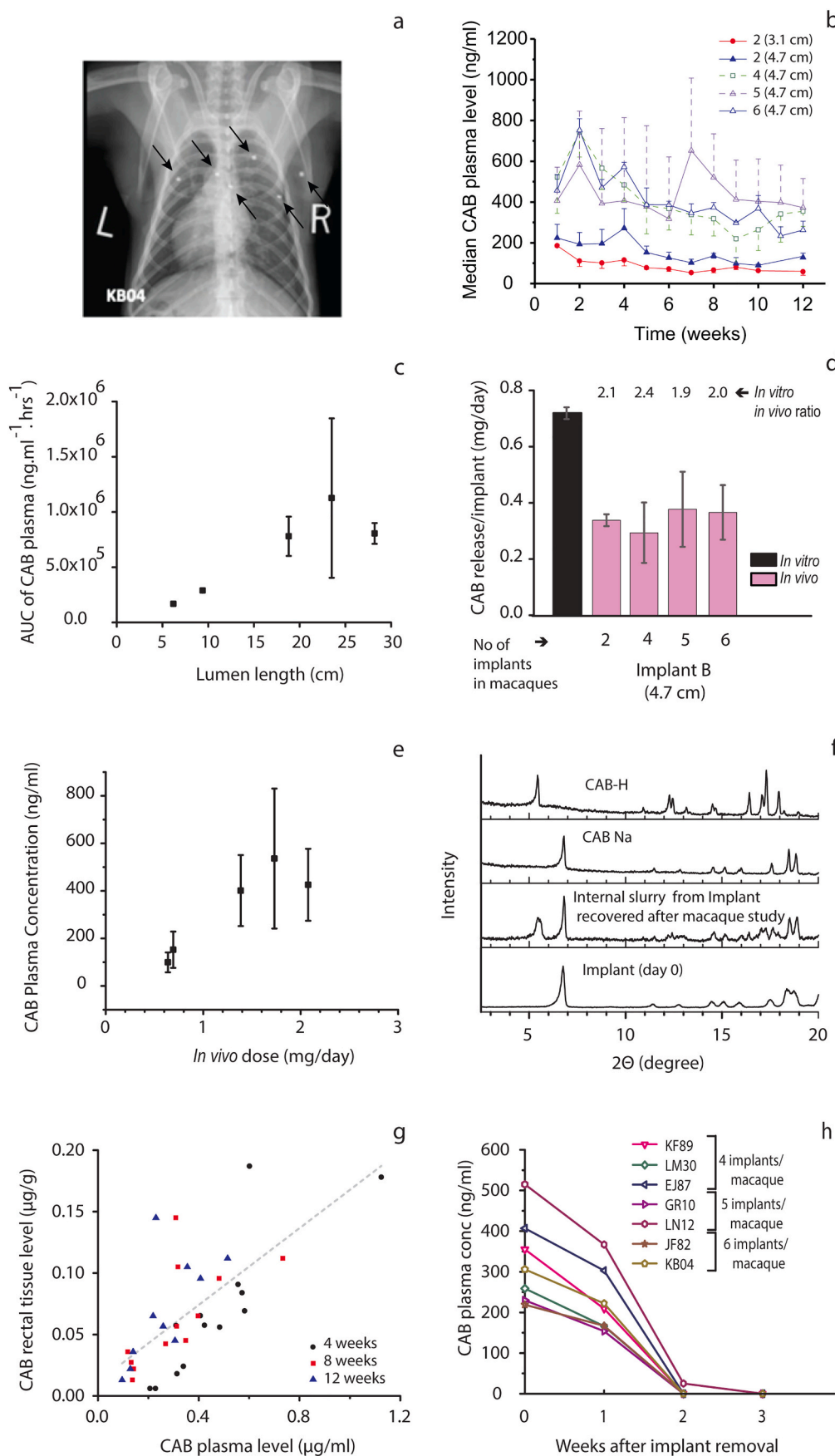


**Fig. 3.** CAB Na implant pharmacokinetics in rhesus macaques. (a) CAB Na Implants containing BaSO<sub>4</sub> imaged in a macaque. Arrows indicate BaSO<sub>4</sub> pellets. (b) Median plasma levels of cabotegravir in macaques with the increasing number of implants, details in Table S1, error bars show interquartile range (c) Cabotegravir exposure versus implant length (d) *in vitro-in vivo* release ratio of implants recovered from NHP, average *in vitro* release rate (*n* = 5) up to day 85 (e) Average cabotegravir plasma level with increasing CAB Na dose calculated from average *in vivo* release rates from explanted implants in each group (f) XRD spectra of contents from an implant recovered after a 12-week macaque study (g) Plasma and rectal cabotegravir levels in macaques (Pearson's *r* = 0.689) (h) Plasma levels of cabotegravir after implant removal in macaques (average plasma *t*<sub>1/2</sub> is approx. 9 days). Error bars, unless otherwise mentioned, are standard deviations.

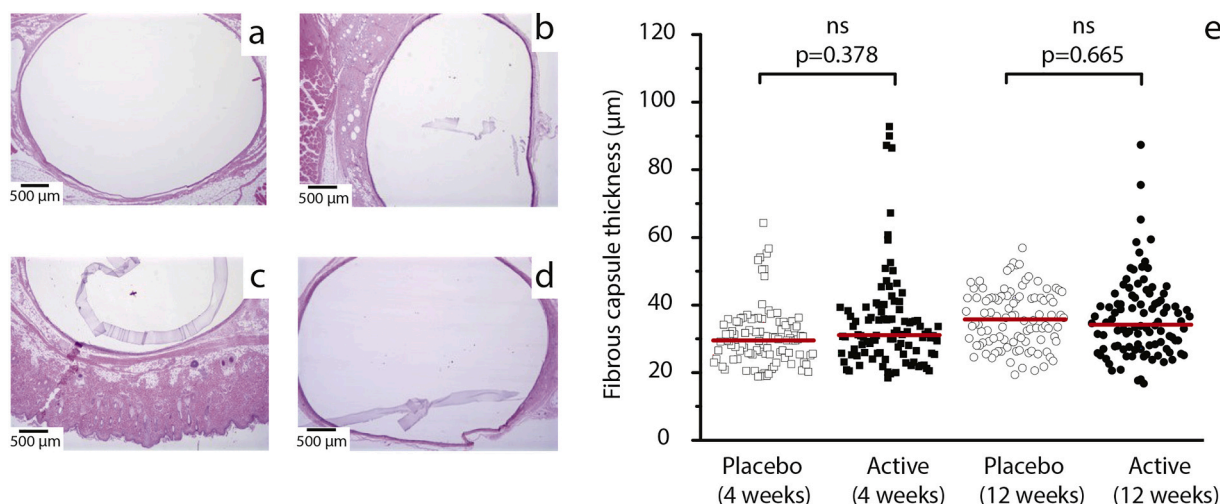


**Fig. 4.** Histological evaluation of cabotegravir implant A and matched placebo. (a, b) 12-week H&E stained slides of placebo implants and two active implants (c, d). In figure b-d the polymer membrane can be seen in the section. Thickness of fibrous tissue capsule,  $N = 100$  measurements from two implants, the horizontal line is the median value.

macaques. In 90 days we observed implant B released 11% of the total cabotegravir load suggesting these implants could deliver cabotegravir for a year in the nonhuman primate model. All components used in this implant have a history of previous human use in parenteral products. The CAB drug loading is high (~87% by weight), allowing efficient use of the implant volume. The methods described are at present capable of reproducibly manufacturing batch sizes up to 1000 implants with common pharmaceutical operations (hot melt extrusion for the RCM tubing and tablet compression for the core pellet) and an impulse sealer. Additionally, this reservoir system design is more complicated and likely more expensive than simple matrix extrusion dosage forms. The cabotegravir release rate is adjustable through the modulation of the geometry and composition of the HPEU HPEU RCM. While the implants generally give reproducible release profiles, disproportionation and counter ion-exchange likely affect transport in complex ways that require further study. Other methods to increase core drug concentration and release rate, like the use of cyclodextrins [25] or high molecular weight pH modifiers, or improved polymers with higher drug diffusivity and solubility may allow improvement in the release rate of cabotegravir from this type of reservoir implant.

#### Acknowledgments

We are grateful to Viiv Healthcare Ltd. for providing cabotegravir to the project. We especially thank Alex Rinehart, Ph.D., William R. Spreen, Pharm.D. from Viiv Healthcare Ltd, and Meredith Clark, Ph.D., from CONRAD for their collective input on this work. Mark Marzinke, Ph.D., from Johns Hopkins University and Meagan Watkins from Tulane University assisted with bioanalytical measurements and the non-human primate studies respectively. We thank Alicia Potuck, Ph.D., from Viiv Healthcare Ltd, for helpful comments on the manuscript. We recognize the use of the IMSERC X-ray Facility at Northwestern University, which has received support from the Soft and Hybrid Nanotechnology Experimental (SHyNE) Resource (NSF ECCS-1542205); the State of Illinois and International Institute for Nanotechnology (IIN). Funding for this work was provided by NIH NIAID grant UM1 A1120184.

#### Appendix A. Supplementary data

Supplementary data to this article can be found online at <https://doi.org/10.1016/j.jconrel.2020.12.024>.

#### References

- [1] L. Osterberg, T. Blaschke, Adherence to medication, *N. Engl. J. Med.* 353 (2005) 487–497.
- [2] J. Trussell, Contraceptive failure in the United States, *Contraception* 83 (2011) 397–404.
- [3] D. Sidebottom, A.M. Ekström, S. Strömdahl, A systematic review of adherence to oral pre-exposure prophylaxis for HIV - How can we improve uptake and adherence? *BMC Infect. Dis.* 18 (2018).
- [4] B.G. Haire, Preexposure prophylaxis-related stigma: strategies to improve uptake and adherence – a narrative review, *HIV/AIDS – Res. Palliat. Care* 7 (2015) 241–249.
- [5] A.S. Fauci, R.R. Redfield, G. Sigounas, M.D. Weahkee, B.P. Giroir, Ending the HIV epidemic: a plan for the United States, *JAMA* 321 (2019) 844–845.
- [6] R.M. Gulick, C. Flexner, Long-acting HIV drugs for treatment and prevention, in: *Annual Review of Medicine*, 2019, pp. 137–150.
- [7] L. Benítez-Gutiérrez, V. Soriano, S. Requena, A. Arias, P. Barreiro, C. de Mendoza, Treatment and prevention of HIV infection with long-acting antiretrovirals, *Expert Rev. Clin. Pharmacol.* 11 (2018) 507–517.
- [8] A.N. Nyaku, S.G. Kelly, B.O. Taiwo, Long-acting antiretrovirals: where are we now? *Curr. HIV/AIDS Rep.* 14 (2017) 63–71.
- [9] D.A. Margolis, M. Boffito, Long-acting antiviral agents for HIV treatment, *Curr. Opin. HIV AIDS* 10 (2015) 246–252.
- [10] M. Gunawardana, M. Remedios-Chan, C.S. Miller, R. Fanter, F. Yang, M. A. Marzinke, C.W. Hendrix, M. Beliveau, J.A. Moss, T.J. Smith, M.M. Baum, Pharmacokinetics of long-acting tenofovir alafenamide (GS-7340) subdermal implant for HIV prophylaxis, *Antimicrob. Agents Chemother.* 59 (2015) 3913–3919.
- [11] E. Schlesinger, D. Johengen, E. Luecke, G. Rothrock, I. McGowan, A. van der Straten, T. Desai, A tunable, biodegradable, thin-film polymer device as a long-acting implant delivering tenofovir alafenamide fumarate for HIV pre-exposure prophylaxis, *Pharm. Res.* 33 (2016) 1649–1656.
- [12] C.Y.X. Chua, P. Jain, A. Ballerini, G. Bruno, R.L. Hood, M. Gupte, S. Gao, N. Di Trani, A. Susnjari, K. Shelton, L.R. Bushman, M. Folci, C.S. Filgueira, M. A. Marzinke, P.L. Anderson, M. Hu, P. Nehete, R.C. Arduino, J.K. Sastry, A. Grattoni, Transcutaneously refillable nanofluidic implant achieves sustained level of tenofovir diphosphate for HIV pre-exposure prophylaxis, *J. Control. Release* 286 (2018) 315–325.
- [13] S.M. Simpson, L. Widanapathirana, J.T. Su, S. Sung, D. Watrous, J. Qiu, E. Pearson, A. Evanoff, D. Karunakaran, J.E. Chacon, P.F. Kiser, Design of a drug-eluting subcutaneous implant of the antiretroviral tenofovir alafenamide fumarate, *Pharm. Res.* 37 (2020) 83.
- [14] S.E. Barrett, R.S. Teller, S.P. Forster, L. Li, M.A. Mackey, D. Skomski, Z. Yang, K. L. Fillgrove, G.J. Doto, S.L. Wood, J. Lebron, J.A. Grobler, R.I. Sanchez, Z. Liu, B. Lu, T. Niu, L. Sun, M.E. Gindy, Extended-duration MK-8591-eluting implant as a candidate for HIV treatment and prevention, *Antimicrob. Agents Chemother.* 62 (2018).
- [15] D. Schürmann, D.J. Rudd, S. Zhang, I. De Lepeleire, M. Robberechts, E. Friedmann, C. Keicher, J. Hüser, J. Hofmann, J.A. Grobler, S.A. Stoch, M. Iwamoto, R. P. Matthews, Safety, pharmacokinetics, and antiretroviral activity of islatravir (ISL, MK-8591), a novel nucleoside reverse transcriptase translocation inhibitor, following single-dose administration to treatment-naïve adults infected with HIV-1: an open-label, phase 1b, consecutive-panel trial, *Lancet HIV* 7 (2020) e164–e172.
- [16] J.M. Anderson, In-vivo biocompatibility of implantable delivery systems and biomaterials, *Eur. J. Pharm. Biopharm.* 40 (1994) 1–8.

- [17] J. Hilborn, L.M. Bjursten, A new and evolving paradigm for biocompatibility, *J. Tissue Eng. Regen. Med.* 1 (2007) 110–119.
- [18] B.A. Johns, T. Kawasuji, J.G. Weatherhead, T. Taishi, D.P. Temelkoff, H. Yoshida, T. Akiyama, Y. Taoda, H. Murai, R. Kiyama, M. Fuji, N. Tanimoto, J. Jeffrey, S. A. Foster, T. Yoshinaga, T. Seki, M. Kobayashi, A. Sato, M.N. Johnson, E.P. Garvey, T. Fujiwara, Carbamoyl pyridone HIV-1 integrase inhibitors 3. A diastereomeric approach to chiral nonracemic tricyclic ring systems and the discovery of dolutegravir (S/GSK1349572) and (S/GSK1265744), *J. Med. Chem.* 56 (2013) 5901–5916.
- [19] W. Spreen, S. Min, S.L. Ford, S. Chen, Y. Lou, M. Bomar, M. St Clair, S. Piscitelli, T. Fujiwara, Pharmacokinetics, safety, and monotherapy antiviral activity of GSK1265744, an HIV integrase strand transfer inhibitor, *Hiv Clin. Trials* 14 (2013) 192–203.
- [20] T. Yoshinaga, M. Kobayashi, T. Seki, S. Miki, C. Wakasa-Morimoto, A. Suyama-Kagitani, S. Kawachi-Miki, T. Taishi, T. Kawasuji, B.A. Johns, M.R. Underwood, E. P. Garvey, A. Sato, T. Fujiwara, Antiviral characteristics of GSK1265744, an HIV integrase inhibitor dosed orally or by long-acting injection, *Antimicrob. Agents Chemother.* 59 (2015) 397–406.
- [21] C. Trezza, S.L. Ford, W. Spreen, R.N. Pan, S. Piscitelli, Formulation and pharmacology of long-acting cabotegravir, *Curr. Opin. HIV AIDS* 10 (2015) 239–245.
- [22] P. Patel, S.L. Ford, Y. Lou, K. Bakshi, A.R. Tenorio, Z. Zhang, R. Pan, W. Spreen, Effect of a high-fat meal on the pharmacokinetics of the HIV integrase inhibitor cabotegravir, *Clin. Pharmacol. Drug Dev.* 8 (2019) 443–448.
- [23] W. Spreen, S.L. Ford, S. Chen, D. Wilfret, D. Margolis, E. Gould, S. Piscitelli, GSK1265744 pharmacokinetics in plasma and tissue after single-dose long-acting injectable administration in healthy subjects, *J. Acquir. Immune Defic. Syndr.* 67 (2014) 481–486.
- [24] T. Kirby, Cabotegravir, a new option for PrEP, *Lancet Infect. Dis.* 20 (2020) 781.
- [25] F.P. Pons-Faudoa, A. Sizovs, N. Di Trani, J. Paez-Mayorga, G. Bruno, J. Rhudy, M. Manohar, K. Gwenden, C. Martini, C.Y.X. Chua, G. Varchi, M.A. Marzinke, A. Grattoni, 2-Hydroxypropyl- $\beta$ -cyclodextrin-enhanced pharmacokinetics of cabotegravir from a nanofluidic implant for HIV pre-exposure prophylaxis, *J. Control. Release* 306 (2019) 89–96.
- [26] D. Cattaneo, C. Gervasoni, Pharmacokinetics and pharmacodynamics of cabotegravir, a long-acting HIV integrase Strand transfer inhibitor, *Eur. J. Drug Metab. Ph.* 44 (2019) 319–327.
- [27] C.D. Andrews, W. Heneine, Cabotegravir long-acting for HIV-1 prevention, *Curr. Opin. HIV AIDS* 10 (2015) 258–263.
- [28] D.A. Margolis, J. Gonzalez-Garcia, H.J. Stellbrink, J.J. Eron, Y. Yazdanpanah, D. Podzamczar, T. Lutz, J.B. Angel, G.J. Richmond, B. Clotet, F. Gutierrez, L. Sloan, M.S. Clair, M. Murray, S.L. Ford, J. Mrus, P. Patel, H. Crauwels, S.K. Griffith, K. C. Sutton, D. Dorey, K.Y. Smith, P.E. Williams, W.R. Spreen, Long-acting intramuscular cabotegravir and rilpivirine in adults with HIV-1 infection (LATTE-2): 96-week results of a randomised, open-label, phase 2b, non-inferiority trial, *Lancet* 390 (2017) 1499–1510.
- [29] S. Ford, B. Stancil, M. Markowitz, I. Frank, R. Grant, K. Mayer, R. Elion, D. Goldstein, C. Fisher, M. Sobieszczyk, G. Joel, H. Van Tieu, W. Weinberg, D. Margolis, K. Hudson, P. Patel, A. Rinehart, K. Smith, W. Spreen, ECLAIR study of cabotegravir LA injections: characterization of safety and PK during the “PK tail” phase, *Aids Res. Hum. Retrov.* 32 (2016) 71.
- [30] G.J. Greene, G. Swann, A.J. Fought, A. Carballo-Diéguez, T.J. Hope, P.F. Kiser, B. Mustanski, R.T. D’Aquila, Preferences for Long-acting Pre-exposure Prophylaxis (PrEP), Daily Oral PrEP, or Condoms for HIV Prevention Among U.S. Men Who Have Sex with Men, *AIDS and Behavior* 21, 2017, pp. 1336–1349.
- [31] T.J. Johnson, M.R. Clark, T.H. Albright, J.S. Nebeker, A.L. Tuitupou, J.T. Clark, J. Fabian, R.T. McCabe, N. Chandra, G.F. Doncel, D.R. Friend, P.F. Kiser, A 90-day tenofovir reservoir intravaginal ring for mucosal HIV prophylaxis, *Antimicrob. Agents Chemother.* 56 (2012) 6272–6283.
- [32] J.T. Su, S.M. Simpson, S. Sung, E. Bryndza Tfaily, R. Veazey, M. Marzinke, J. Qiu, D. Watrous, L. Widanapathirana, E. Pearson, M.M. Peet, D. Karunakaran, B. Grasperge, G. Dobek, C.M. Cain, T. Hope, P.F. Kiser, A subcutaneous implant of tenofovir alafenamide fumarate causes local inflammation and tissue necrosis in rabbits and macaques, *Antimicrob. Agents Chemother.* (2019) (AAC.01893-01819).
- [33] L.M. Johnson, S.A. Krovi, L. Li, N. Girouard, Z.R. Demkovich, D. Myers, B. Creelman, A. van der Straten, Characterization of a reservoir-style implant for sustained release of tenofovir alafenamide (TAF) for HIV pre-exposure prophylaxis (PrEP), *Pharmaceutics* 11 (2019) 315.
- [34] C.A. Schneider, W.S. Rasband, K.W. Eliceiri, NIH image to ImageJ: 25 years of image analysis, *Nat. Methods* 9 (2012) 671–675.
- [35] FDA, Dissolution Testing of Immediate Release Solid Oral Dosage Forms, 1997.
- [36] V.P. Shah, Y. Tsong, P. Sathe, J.P. Liu, In vitro dissolution profile comparison-statistics and analysis of the similarity factor, *f2*, *Pharm. Res.* 15 (1998) 889–896.
- [37] B.V. Robinson, F.M. Sullivan, J.F. Borzelleca, S.L. Schwartz, PVP: A Critical Review of the Kinetics and Toxicology of Polyvinylpyrrolidone (Povidone), 1990.
- [38] M.B. Lowinger, S.E. Barrett, F. Zhang, R.O. Williams, Sustained release drug delivery applications of polyurethanes, *Pharmaceutics* 10 (2018) 55.
- [39] K.S. Taskar, A. Patel, S.J. Cozens, H. Tracey, S. Ford, K. Han, W. Spreen, M. Baker, P. Patel, Prediction of renal OAT1 and OAT3 inhibition by cabotegravir using PBPK modelling [CROI abstract 470]. In special issue: abstracts from the 2019 conference on retroviruses and opportunistic infections, *Topics Antiviral Med.* 27 (Suppl. 1) (2019).
- [40] C.D. Andrews, W.R. Spreen, H. Mohri, L. Moss, S. Ford, A. Gettie, K. Russell-Lodrigue, R.P. Bohm, C. Cheng-Mayer, Z. Hong, M. Markowitz, D.D. Ho, Long-acting integrase inhibitor protects macaques from intrarectal simian/human immunodeficiency virus, *Science* 343 (2014) 1151–1154.
- [41] C.D. Andrews, Y.L. Yueh, W.R. Spreen, L. St Bernard, M. Boente-Carrera, K. Rodriguez, A. Gettie, K. Russell-Lodrigue, J. Blanchard, S. Ford, H. Mohri, C. Cheng-Mayer, Z. Hong, D.D. Ho, M. Markowitz, A long-acting integrase inhibitor protects female macaques from repeated high-dose intravaginal SHIV challenge, *Sci. Transl. Med.* 7 (2015).
- [42] International Organization for Standardization, Biological Evaluation of Medical Devices - Part 6: Tests for Local Effects after Implantation (ISO 10993-6:2016), International Organization for Standardization, Geneva, Switzerland, 2016, p. 29.